Verification of a Frequency Dispersion Model in the Performance of a GaAs pHEMT Travelling-Wave MMIC

I. Kallfass[1], C. Zhang[1], J. Grünenpütt[2], C. Teyssandier[3], H. Schumacher[1]
[1]Department of Electron Devices and Circuits, University of Ulm
Albert-Einstein-Allee 45, 89069 Ulm, Germany
[2]United Monolithic Semiconductors GmbH, Ulm, Germany
[3]United Monolithic Semiconductors SAS, Orsay, France
email: ikall@ebs.e-technik.uni-ulm.de

***Abstract*— The impact of frequency dispersive effects on typical figures of merit is investigated in a distributed MMIC realized in 0.15μm GaAs pHEMT technology. A novel compact dispersion model, allowing for accurate simulation of both static and dynamic multiple time constant IV characteristics, is employed. In a comparison of measurement and simulation, the model is both validated and used to quantify and interpret the error introduced when neglecting frequency dispersion in the design of MMICs. Device operation is investigated with respect to gain, linearity and power-added efficiency, all of them affected by dispersion effects. The model is shown to significantly improve simulation accuracy by increasing the validity range in terms of the frequency- and voltage regimes.**

I. Introduction

Today's high-performance hetero field-effect transistor (HFET) technologies show significant dispersive effects, mainly affecting the device's current-voltage (IV) characteristics by causing a frequency- or time dependence to drain current. The physical effects responsible for dispersion in these devices are thermal- or self-heating effects, trapping and de-trapping of carriers, interface- and surface state occupation as well as impact ionization. All of the above mentioned effects can empirically be described by their quantitative impact on device characteristics and an associated time constant or corner frequency.

State-of-the-art modelling of frequency dispersion is generally focusing on the physical description of one particular effect. Thermal models incorporate temperature as a circuit parameter [1], [2] and use a parallel R-C thermal subcircuit to compute a change in drain current as a function of instantaneous power consumption. Time-dependent interface charges are identified to cause dispersion in GaN HFETs [3], while thermal and trap-related modelling of dispersion has been carried out e.g. for GaN MESFET devices [4]. Here, a widely used dispersion model topology combines static and dynamic current sources via a DC-blocking capacitor [5], [6]. Another empirical approach to modelling dispersion is the use of equivalent voltage sources in the FET circuit topology [7]. On the system level, frequency dispersion is responsible for memory effects and treated by behavioural modelling [8], [9].

In this paper, we present a novel empirical dispersion model on the device level, dedicated to the efficient use in broadband circuit design. It features accurate description of devices exhibiting different dispersion effects, taking into account their respective time constants as well as impact on IV characteristics. The model is used to investigate the influence of dispersion on the performance of a travelling-wave MMIC [10], designed and fabricated using a 150nm GaAs pHEMT technology whose active devices have an f_T of 75 GHz. Cascode amplifier cells with variable current-voltage feedback, realized by a FET biased in its linear operating region, are used in an eight-stage distributed circuit configuration (Fig. 1). In- and output of the cascodes as well as the feedback transistor gate are embedded into inductive microstrip lines, forming artificial 50Ω transmission lines and leading to the well-known bandwidth enhancement of travelling-wave circuits.

By applying a local oscillator drive to the feedback line the device may be operated as a mixer, exhibiting measured conversion loss of 2dB in a bandwidth exceeding 50GHz. Variable gain amplification is obtained by applying a controlling bias to the feedback line. The gain can be controlled between 5-12dB with a near-constant bandwidth of up to 43GHz.

The current-voltage feedback topology is particularly challenging for the model quality both in terms of small- and large signal analysis as well as frequency dispersion. It uses a scaled transistor biased in its linear operating region to obtain the

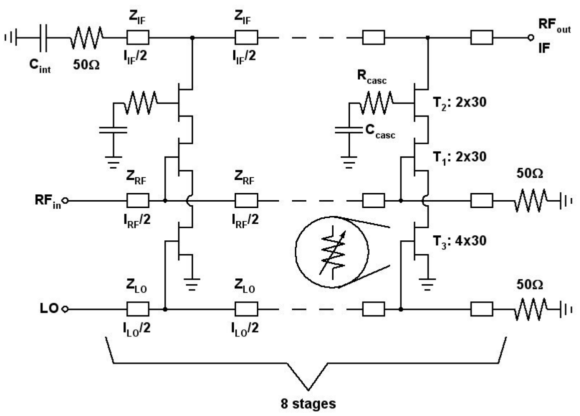

Fig. 1. Distributed circuit topology for mixer and VGA operation. Eight cascode stages with resistive source feedback are embedded into inductive transmission lines.

feedback effect. Here, dispersion effects show significant differences between static and dynamic IV characteristics. For small-signal analysis, an accurate prediction of the bias situation is required in order to linearize the device in a region where both its trans- and output conductance are highly nonlinear. Under large-signal conditions, e.g. for mixer operation, the feedback FET is driven between linear-, knee- and saturated regimes. Additionally, evaluation of amplifier linearity requires the device model to be accurate primarily with respect to the cascode class A operation.

In the comparison of measurement and simulation, the presented model is generally verified. It allows for accurate simulation of characteristics affected by frequency dispersion. Finally, the dispersion model is compared to simulation results obtained from purely static and dynamic models.

II. The Dispersion Model

Basis of the drain current model is the physically well-founded assumption that individual dispersion effects introduce an exponentially decaying time domain step response of drain current. In the frequency domain, this results in a single-pole transfer function. The topology employed to achieve such dispersion characteristics is shown in Fig. 2. A static nonlinear current source I_0 is combined in parallel with dynamic sources, realized by voltage controlled current sources whose nonlinear characteristics result from an auxiliary L-R circuit. In the following, dynamic characteristics obtained from a measurement excluding dispersion effects with time constant τ_i are denoted I_i.

The total drain current can be written as

$$I_{ds} = I_0 + \sum_{i=1..n} I_{xi} \frac{j\omega L_{xi}}{R_x + j\omega L_{xi}} \qquad (1)$$

where n is the number of dispersion sources and $I_{xi} = I_i - I_{i-1}, i = 1..n$ is the current attributed to dispersion source i. The nonlinear currents I_i represent the dynamic current characteristics obtained e.g. from pulsed-IV measurements. The parallel placement of several dispersion sources will lead to a total drain current in the frequency domain of I_i for $f_i < f < f_{i+1}$where $\tau_i = \frac{1}{2\pi f_i} = \frac{L_{xi}}{R_{xi}}$ are the time constants and corner frequencies of the individual dispersion sources.

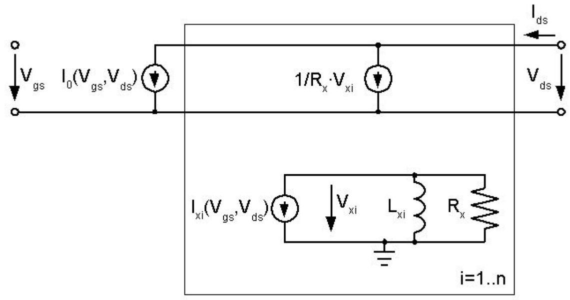

Fig. 2. Device-level dispersion model for multiple time constant drain current characteristics. The dispersion part is embedded into a conventional HFET circuit topology.

This model improves conventional R-C type topologies with respect to accuracy and computational efficiency. Mainly, however, it adds the multiple time constant functionality. All nonlinear drain current characteristics, i. e. static (I_0) and multiple dynamic (I_i) sources, are described using a modified COBRA expression [11], [12].

The model employed in the present work uses the static drain current combined with two dispersion sources resulting from pulsed-IV measurements. One based on pulses with $100ns$ width, and a second with $2\mu s$ pulse width. Pulse spacing of both measurements is $1ms$ with a device quiescent condition for maximum gain. It can be shown that the resulting IV characteristics of the $2\mu s$ pulse measurement exclude a slow dispersion effect, usually associated with self-heating, while the $100ns$ pulses allow to exclude a second, faster dispersion effect, usually associated with trapping effects. The resulting characteristics are shown in Fig. 3. The on-wafer, pulsed-IV measurement setup uses a DIVA D225 dynamic IV analyzer from Accent Optical Technologies.

The dispersion part of the model is embedded into a conventional HFET equivalent circuit containing nonlinear gate capacitance and -current models [12], and is fully implemented as a scalable "user-compiled" model into the ADS simulation environment. To demonstrate correct operation of the dispersion model, it is used in a transient simulation to predict the drain current response to a step change in operating conditions. Fig. 4

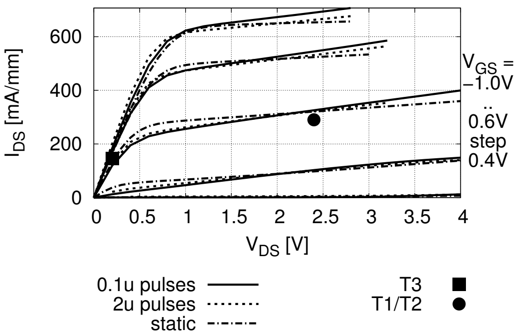

Fig. 3. Static and dynamic drain current characteristics in a 2x50μm device. Dynamic characteristics are obtained from pulsed-IV measurements with 100ns and 2μs pulse widths.

shows measured and modelled transient responses of a 2x20μm device being pulsed from an active quiescent condition into the linear- and high power region. Measurements are obtained by plotting the instantaneous drain current from pulsed-IV characterisation versus pulse width. They reveal exponentially decaying responses with two time constants, $\tau_1 = 200\mu s$ and $\tau_2 = 1\mu s$. As can be seen, the model is capable of describing the time dependent current together with the transition between the different dispersion regimes. Furthermore, the dynamic sources can be disabled, and purely static or dynamic characteristics can be attributed to the main current source I_0. This allows for an evaluation of the error introduced by neglecting frequency dispersion.

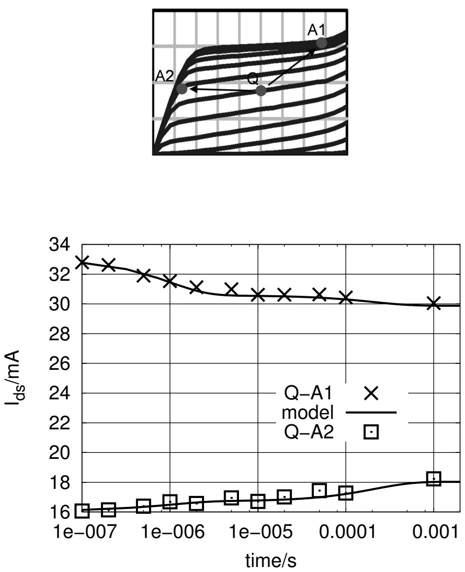

Fig. 4. Measured and modelled transient response of drain current in a 2x20μm device being pulsed from quiescent condition Q into bias points A1 and A2.

III. Device Characteristics

A. Amplifier Gain and Mixer Conversion Loss

Fig. 5 shows measured amplifier gain as well as conversion loss of the mixer operated both with fixed f_{IF} of 2GHz and fixed f_{LO} of 25GHz. The simulation accuracy of the dispersion model is within 1dB for all values. The purely static model deviates by another 0.5dB in gain prediction. In a travelling-wave amplifier, the total gain depends on the losses introduced to the drain line by the non-ideal output conductance of the individual amplifier stages. The purely static model introduces an error of more than 50% (2.3mS instead of 4.8mS) to output conductance, as evidenced in Fig. 3 which shows the operating condition of the cascode transistors T1/T2.

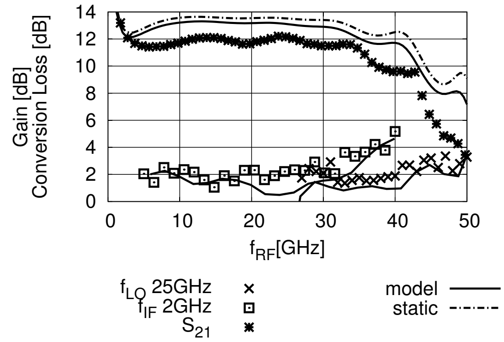

Fig. 5. The comparison of measured and simulated gain and conversion loss validates the device model.

B. Gain compression and PAE

The simulation of power-added efficiency (PAE) at microwave frequencies requires the static model to predict current consumption (134mA measured, 131mA simulated). The dynamic part is responsible for gain and gain compression. Also, the dynamic signal introduces a self-biasing effect, which in turn is affecting the static characteristics. Fig. 6 shows PAE at 10GHz f_{RF} and confirms that only the dispersion model is capable of accurately predicting both maximum PAE and the associated input power.

C. Gain versus Control Voltage

Fig. 7 shows small-signal gain versus control voltage (gate bias of feedback transistor T3) at 25GHz f_{RF}. The purely dynamic model's prediction deviates from measurements when T3 is biased in regions of large differences between static and dynamic characteristics (see bias in Fig. 3). The static model deviates both in gain and in gain reduction

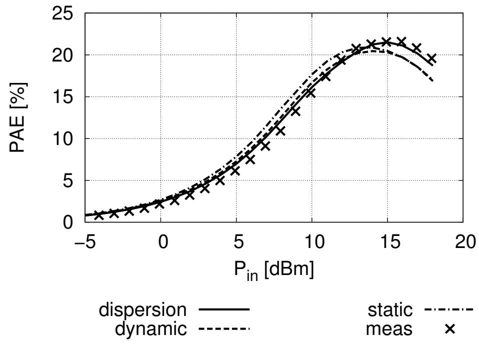

Fig. 6. Linearity simulations, here PAE at 10GHz, rely on a dispersion model which is accurate both in static- and dynamic analysis.

with control bias since it undervalues the feedback effect resulting from the output conductance of T3.

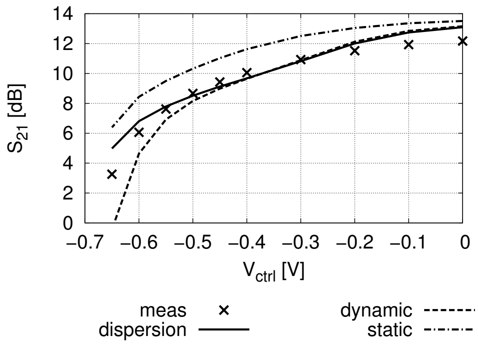

Fig. 7. Amplifier gain versus control voltage at 25GHz. Only the full dispersion model is capable of predicting correct gain in different bias regimes.

IV. Conclusion

Circuit design employing dispersive technologies is shown to be significantly improved by using the proposed circuit level dispersion model. Excellent agreement with measurements is reached over a wide range of bias conditions as well as for static- and dynamic figures of merit.

References

[1] C.J. Wei, Y. A. Tkachenko, D. Bartle, “Table-based Dynamic FET Model Assembled From Small-Signal Models,” *IEEE Trans. Microwave Theory and Techniques*, vol. 47, pp. 700–705, June 1999.

[2] Y. Yang, Y.Y. Woo, J. Yi, B. Kim, “A New Empirical Large-Signal Model of Si LDMOSFETs for High-Power Amplifier Design,” *IEEE Trans. Microwave Theory and Techniques*, vol. 9, pp. 1626–1633, September 2001.

[3] R. Vetury, N. Q. Zhang, S. Keller, U. K. Mishra, “The Impact of Surface States on the DC and RF Characteristics of AlGaN/GaN HFETs,” *IEEE Trans. Electron Devices*, vol. 48, pp. 560–566, March 2001.

[4] S.S. Islam, A. F. M. Anwar, “Self-Heating and Trapping Effects on the RF Performance of GaN MESFETs,” *IEEE Trans. Microwave Theory and Techniques*, vol. 52, pp. 1229–1236, April 2004.

[5] J.W. Lee, K.J. Webb, “A Temperature-Dependent Nonlinear Analytic Model for AlGaN-GaN HEMTs on SiC,” *Trans. Microwave Theory and Techniques*, vol. 52, pp. 2–9, January 2004.

[6] J.M. Golio, M.G. Miller, G.N. Maracas, D.A.Johnson, “Frequency-Dependent Electrical Characteristics of GaAs MESFETs,” *Trans. Electron Devices*, vol. 37, pp. 1217–1227, May 1990.

[7] A. Santarelli, G. Zucchelli, R. Paganelli, G. Vannini, F. Filicori, “Equivalent-Voltage Description of Low-Frequency Dispersive Effects in Large-signal FET Models,” *Proc. GaAs Symposium, European Microwave Week London*, September 2001.

[8] V. Rizzoli, D. Masotti, F. Mastri, “Behavioural Modelling of Thermally Induced Distortion in RF/Microwave Nonlinear Subsystems,” *Proc. 34th EuMC Amsterdam*, pp. 845–848, 2004.

[9] H. Ku, J.S. Kenney, “Behavioral Modeling of Nonlinear RF Power Amplifiers Considering Memory Effects,” *IEEE Trans. Microwave Theory and Techniques*, vol. 51, pp. 2495–2504, December 2003.

[10] I. Kallfass, H. Schumacher, T. Purtova, A. Brokmeier, W. Ludwig, “One single travelling-wave MMIC for highly linear broadband mixers and variable gain amplifiers,” *IMS, Long Beach*, June 2005.

[11] V. I. Cojocaru, T. J. Brazil, “A Scalable General-Purpose Model for Microwave FET’s Including DC/AC Dispersion Effects,” *IEEE Trans. Microwave Theory and Techniques*, vol. 45, pp. 2248–2255, December 1997.

[12] I. Kallfass, C. Schick, H. Schumacher, T. J. Brazil, “A Universal Large-Signal Model for Hetero Field-Effect Transistors,” *Proc. 12th GaAs Symposium, European Microwave Week, Amsterdam, Netherlands*, October 2004.